Reconstruction of particle-size distributions from light-scattering patterns using three inversion methods

Javier Vargas-Ubera, J. Félix Aguilar, and David Michel Gale

By means of a numerical study we show particle-size distributions retrieved with the Chin–Shifrin, Phillips–Twomey, and singular value decomposition methods. Synthesized intensity data are generated using Mie theory, corresponding to unimodal normal, gamma, and lognormal distributions of spherical particles, covering the size parameter range from 1 to 250. Our results show the advantages and disadvantages of each method, as well as the range of applicability for the Fraunhofer approximation as compared to rigorous Mie theory.

OCIS codes: 290.0290, 290.3200, 290.4020, 290.5850.

1. Introduction

Light scattering as a diagnostic tool has proved to be a suitable technique for resolving real problems of increasing complexity in the area of particle sizing. This technique has inherent problems, however, owing to the need to perform a large number of numerical calculations to resolve the inverse problem generated by the rigorous solution for spherical particles as described by Mie theory[1] and the need to input the refractive indices of the materials being measured.

An alternative formalism to Mie theory is the Fraunhofer approximation, which is based on scalar diffraction theory. This approximation is valid for particles of radius greater than 2.5 μm when analyzed with visible light, wavelength $\lambda = 0.5$ μm.[2] Jones[3] proposed that, for nonabsorbent particles with a radius greater than 1.5 μm, a refractive index greater than 1.3 and for errors below 20%, the Fraunhofer approximation is valid for visible wavelengths.

Although Mie theory is valid in the region of radii and wavelengths where the Fraunhofer approximation may be used, it is important to compare both techniques and obtain a criterion that allows us to decide when it is appropriate to use Fraunhofer since numerical calculations using Mie theory become extremely slow as the particle size increases. Additionally one should consider the more general case of a conglomerate of particles of varying sizes, which more closely resembles real-world sizing tasks. One should thus determine if the validity criterion depends on the type of distribution and the inversion method used to retrieve the particle-size distribution (PSD).

We use normal, gamma, and lognormal distributions to numerically simulate an intensity pattern using Mie theory. For the inverse problem of PSD recovery, we use the Chin–Shifrin (CS) method[4–9] and the singular value decomposition (SVD) technique,[9–12] when working with the Fraunhofer approximation, and the Phillips–Twomey (PT) method[12,13] and the SVD technique when using Mie theory. These inversion methods are widely used at present. Stochastic numerical techniques such as the Monte Carlo method[14] and genetic algorithms[15,16] have been reported elsewhere and are not considered in this work.

In the Section 2 we present some general considerations of importance to the subsequent numerical simulations. The kernels for the Fraunhofer approximation and Mie theory are presented in Section 3, and the CS, SVD, and PT numerical techniques are introduced. Section 4 shows the results relating to the critical size interval that defines the validity of the Fraunhofer approximation that applies typically to these monomodal distributions with the CS and SVD inversion methods. In Section 5 results are given for Mie theory by using SVD and PT methods. The regularization parameter, which affects the performance of the PT method, is discussed in Section 6, and a

The authors are with the Instituto Nacional de Astrofísica Óptica y Electrónica (INAOE), Luis E. Erro No. 1, Tonantzintla Puebla 72840, México. J. Vargas-Ubera's e-mail address is thesis_234@yahoo.es.

Received 10 July 2006; accepted 28 August 2006; posted 12 September 2006 (Doc. ID 72843); published 15 December 2006.

0003-6935/06/010124-09$15.00/0

comparison between Mie and Fraunhofer with their respective inversion methods for large particles is presented in Section 7. Our conclusions are presented in Section 8.

2. General Considerations

The gamma and lognormal distributions used in this work are those used frequently to model PSDs in aerosols.[17] The gamma distribution is defined as

$$f_G(\alpha) = \begin{cases} N \dfrac{(\alpha - \alpha_0)^{(1/b)-3}}{(bt)^{(1/b)-2}\Gamma^{[(1/b)-2]}} \exp\left[\dfrac{\alpha_0 - \alpha}{bt}\right] & \text{for } \alpha > \alpha_0 \\ 0 & \text{for } \alpha \le \alpha_0 \end{cases}, \tag{1}$$

where $\alpha = kr$ is a nondimensional quantity known as the size parameter for a particle of radius r, $k = 2\pi/\lambda$ is the wavenumber, and λ is the wavelength of light in the medium that surrounds the particles. Quantities t and b are the effective size parameter and the variance, respectively, and control the shape of the distribution.[5] Finally, α_0 determines the smallest size parameter present in the distribution, N is the total number of particles, and Γ is the gamma function.

The lognormal distribution is defined as

$$f_L(\alpha) = \frac{N}{\sigma(\alpha - \alpha_0)\sqrt{2\pi}} \exp\left[-\left(\frac{\ln\left(\dfrac{\alpha - \alpha_0}{A_0}\right)}{\sigma\sqrt{2}}\right)^2\right], \tag{2}$$

where N and α_0 are as defined for the gamma distribution, σ is the standard deviation of the distribution, and A_0 is a quantity related to the mean size parameter (μ) of a normal distribution through

$$\mu = \exp\left[\ln(A_0) + \frac{\sigma^2}{2}\right]. \tag{3}$$

A third distribution used in this work is the normal distribution, which facilitates interpretation of the results when attempting to establish a critical interval of validity for the Fraunhofer approximation. It serves as a reference point with respect to the gamma and lognormal distributions, which are in general asymmetric, and it helps us to evaluate the quality of the retrieval for each inversion method used. The normal distribution is defined as

$$f_N(\alpha) = \frac{N}{\sigma\sqrt{2\pi}} \exp\left[-\frac{1}{2}\left(\frac{\alpha - \mu}{\sigma}\right)^2\right], \tag{4}$$

where μ, σ, and N are the mean size parameter, the standard deviation, and the number of particles, respectively.

In the rigorous simulations of intensity we use the relative refractive index $m = n_p/n_m = 1.5$, where n_p and n_m are the indices of refraction of the particle and the surrounding medium, respectively.

The total scattered intensity, $I(\theta)$, attributable to a given proposed distribution $f(\alpha)$, is defined by the following integral equation[1]:

$$I(\theta) = \int_0^\infty I(\theta, \alpha) f(\alpha) \mathrm{d}\alpha, \tag{5}$$

where θ is the forward-scattering angle in the direction of propagation. The kernel, $I(\theta, \alpha)$, represents the scattered intensity in the annular region defined by angle θ, corresponding to a single particle with size parameter α and is calculated according to Mie theory. $f(\alpha)$ is the particle density, such that $f(\alpha)\mathrm{d}\alpha$ is the number of particles with sizes between α and $\alpha + \mathrm{d}\alpha$.

The integral in Eq. (5) is calculated numerically by using the trapezoidal rule in the finite interval in which the proposed distribution is defined. If the distribution of particles $f(\alpha)$ is discretized into M size intervals, then for the most general case the total intensity of Eq. (5) is reduced to a system of linear equations that gives rise to a matrix equation of the form

$$\mathbf{y} = \mathbf{A}\mathbf{x}, \tag{6}$$

where $\mathbf{y}$ is the total intensity vector due to the contribution of each size interval at a given angle θ, $\mathbf{A}$ is a matrix that contains the scattering coefficients a_{ij}, calculated according to Mie theory or Fraunhofer approximation as appropriate, and $\mathbf{x}$ is the unknown vector that contains the fraction of particles in each size interval.

Normally in such problems matrix $\mathbf{A}$ is almost singular or ill-conditioned, and a direct inversion using common methods such as lower triangular–upper triangular (LU) decomposition or Gaussian elimination, usually produces nonphysical solutions. For this reason one must turn to numerical inversion methods adequate for this type of matrix.

3. Kernel and Inversion Methods

In the Fraunhofer approximation the kernel $I(\theta, \alpha)$ is modeled as the Airy pattern produced by an opaque disk of radius r equal to that of the particle. Hence from Eq. (5) the total intensity is given by[1]

$$I(\theta) = \frac{I_0}{k^2 F^2} \int_0^\infty \frac{\alpha^2 J_1^{\,2}(\alpha\theta)}{\theta^2} f(\alpha)\mathrm{d}\alpha, \tag{7}$$

where I_0 is the incident beam intensity, J_1 is a Bessel function of the first kind, first order, and F is the focal length of the receiver lens, as typically encountered in laser diffraction particle size analyzers. This equation accepts an asymptotic analytic solution, widely

referred to in the literature as the CS method[6,9]

$$f(\alpha) = \frac{-2\pi k^3 F^2}{\alpha^2} \int_0^\infty (\alpha\theta) J_1(\alpha\theta) Y_1(\alpha\theta) \frac{\mathrm{d}}{\mathrm{d}\theta}\left[\theta^3 \frac{I(\theta)}{I_0}\right] \mathrm{d}\theta, \tag{8}$$

where, Y_1 is a Bessel function of the second kind, first order. This solution has differences in the sampling and size dominions, and this leads to serious problems in the retrieval of the function. More precisely, angle θ can acquire values only in a small interval, limited by the validity of the paraxial approximation, up to a maximum angle θ_{max}, and this has important implications in the discretization of the integral. Further problems are encountered with the angular sampling interval $\Delta\theta$ and the minimum sampling angle θ_{min}, and furthermore, this solution is applicable only for particles whose radii are several times greater than the analyzing wavelength.

The second inversion method, SVD, is applicable to both Fraunhofer and Mie theories. It consists of resolving the inverse problem posed by Eq. (6) using the factorization of range p of matrix $\mathbf{A}(m \times n)$ into two orthonormal matrices, $\mathbf{U}(m \times p)$, $\mathbf{V}(n \times p)$, and a diagonal matrix $\mathbf{P}(p \times p)$, such that

$$\mathbf{A} = \mathbf{U}\mathbf{P}\mathbf{V}^{\mathbf{T}}, \tag{9}$$

$$\mathbf{Q} = \mathbf{A}^{-1} = \mathbf{V}\mathbf{P}^{-1}\mathbf{U}^{\mathbf{T}}. \tag{10}$$

All the diagonal elements of matrix $\mathbf{P}$ are positive and are known as singular values. The degree of singularity in $\mathbf{A}$ is determined by the condition number, the ratio between the largest and the smallest singular values. Furthermore, if the pseudoinverse matrix of $\mathbf{A}$ generated by SVD is $\mathbf{Q}$, then the solution to the inverse problem presented in Eq. (6) is

$$\mathbf{x} = \mathbf{Q}\mathbf{y}. \tag{11}$$

To introduce the third inversion method, we now consider the kernel for spherical particles within the context of Mie theory. From Eq. (5) the total intensity is[1]

$$I(\theta) = \int_0^\infty \frac{I_0(i_1 + i_2)}{2k^2R^2} f(\alpha)\mathrm{d}\alpha, \tag{12}$$

where i_1 and i_2 refer to the intensity of light vibrating perpendicular and parallel to the reference plane, respectively. Information about particle size and relative refractive index m is contained in these intensity contributions. R is the distance from the particle to the plane of observation.

Here it is important that we apply an adequate inversion method so as to obtain the maximum efficiency in calculating the inverse matrix that resolves the inherent ill-conditioned behavior in the inverse problem expounded by Eq. (12). A common strategy to obtain a stable solution is to incorporate *a priori* information pertaining to the desired result. A widely used technique, known as the Tikhonov regularization[12] and also referred to as the PT method,[13] offers this possibility.

The PT method postulates a minimization problem, which in a least-squares sense can be written in the form

$$\|\boldsymbol{\epsilon}\|^2 + \gamma^2\|\mathbf{B}\mathbf{x}\|^2 \rightarrow \min. \tag{13}$$

Here, $\boldsymbol{\epsilon} \equiv \mathbf{A}\mathbf{x} - \mathbf{y}$ is the residual vector, $\|\cdot\|$ denotes the Euclidian norm, and $\mathbf{B}$ is a matrix operator designed to reduce the ill-conditioned behavior of matrix $\mathbf{A}$. Generally, $\mathbf{B}$ is a finite-differential operator of second order that has a smoothing effect on $\mathbf{x}$ and is included as *a priori* information about the distribution sought. The γ parameter represents an adjustable regularization parameter or Lagrange multiplier; it is a real and positive number, and it is also a weight factor for the included *a priori* information.

For a given value of γ, from Eq. (13) one achieves a unique solution given by[13]

$$\mathbf{x} = (\mathbf{A}^{\mathbf{T}}\mathbf{A} + \gamma\mathbf{H})^{-1}\mathbf{A}^{\mathbf{T}}\mathbf{y}, \tag{14}$$

where $\mathbf{H} = \mathbf{B}^{\mathbf{T}}\mathbf{B}$ serves as the regularization matrix to suppress spurious oscillations that appear in the solution vector of the basic linear system [Eq. (6)], which is ill-conditioned.

Finally, the inverse matrix $(\mathbf{A}^{\mathbf{T}}\mathbf{A} + \gamma\mathbf{H})^{-1}$ may be calculated by using standard techniques; for this work we use LU decomposition.

Although γ must be determined to solve the inverse problem, an initial proposal for the value of the regularization parameter is suggested,[12] since γ is constant in the minimization problem of Eq. (13). This initial value is given by

$$\gamma_0 = \frac{\mathbf{Tr}(\mathbf{A}^{\mathbf{T}}\mathbf{A})}{\mathbf{Tr}(\mathbf{H})}, \tag{15}$$

since this choice tends to make the two parts of the minimization have comparable weights. We can adjust from there until we reach a good match between the proposed and the retrieved distributions. Details of the proper selection of γ are discussed in Section 6.

4. Validity Range in the Fraunhofer Approximation: Comparison between the Chin–Shifrin Method and the Singular Value Decomposition Technique

Taking as a premise the results of Hodkinson[2] and Jones,[3] we consider a critical interval for the study of

Table 1. Parameters of the Proposed Distribution Functions[a]

Normal		Gamma		Lognormal	
μ	σ	t	b	A_0	σ
50	15	55	0.5	52	2.2
45	15	55	0.7	45	2.8
40	15	50	0.8	42	3.0
35	15	45	0.8	37	3.0
30	15	40	1.1	33	3.8

[a]The size dominion $1 \leq \alpha \leq 100$ is used throughout. Sampling $\Delta\alpha = 1$; minimum sampling angle $\theta_{min} = 0.057°$; angular sampling $\Delta\theta = 0.057°$; and maximum sampling angle $\theta_{max} = 10°$.

the behavior of the Fraunhofer approximation, using five characteristic size ranges for each of the three distribution types. The five normal distributions are centered at size parameters $\alpha = 50$, 45, 40, 35, and 30, with a standard deviation $\sigma = 15$ used throughout. The corresponding gamma and lognormal distributions have modal peaks in the same vicinity as that of the normal distributions. The distribution parameters are shown in Table 1. The size dominion for all distributions is $1 \leq \alpha \leq 100$, with the same sampling interval $\Delta\alpha = 1$. It is sufficient to consider just the distributions centered at the extremes of the modal size interval since they illustrate adequately the behavior of the intensity patterns and the recuperation tendency.

Figure 1(a) shows a normal distribution centered at $\alpha = 50$ with a standard deviation of $\sigma = 15$, together with gamma and lognormal distributions centered within the same interval close to $\alpha = 50$. Figure 1(b) compares the logarithm of the intensity patterns

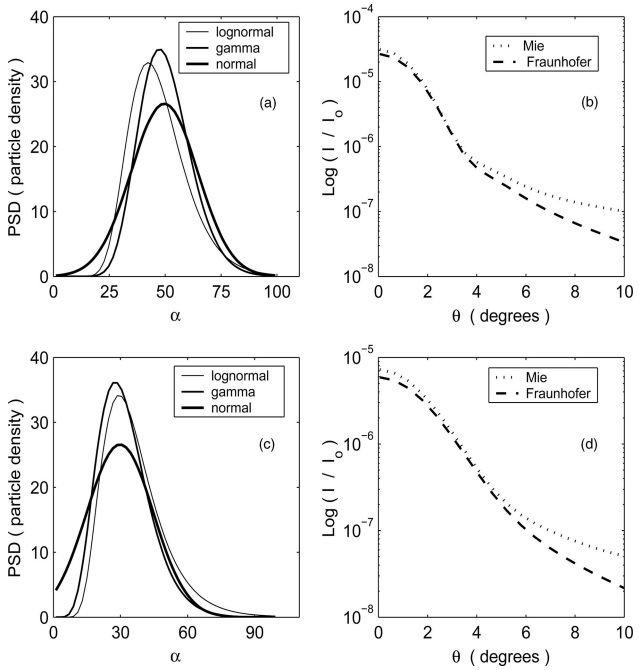

Fig. 1. (a), (c) Normal, gamma, and lognormal distributions centered at $\alpha \sim 50$ and $\alpha \sim 30$, respectively. (b), (d) Intensity patterns for the normal distribution of (a) and (c), respectively.

(normalized with total incident intensity) calculated by using Fraunhofer and Mie theory [Eqs. (7) and (12)] for just the normal distribution, since the gamma and lognormal distributions generate identical patterns. Figure 1(c) shows the three distributions centered at $\alpha = 30$. The resulting intensity patterns, again for only the normal distribution, are shown in Fig. 1(d).

For the following analysis we consider the six distributions of Figs. 1(a) and 1(c) as representative of the extremes of interval that we consider critical for the validity of the Fraunhofer approximation. Thus on referring to the critical interval, we refer to the modal values in the interval of size parameter that delimits these distributions.

The intensity patterns calculated using the Fraunhofer approximation and Mie theory for a single distribution are in agreement for small angles but show discrepancies at larger angles. The angular region in which these discrepancies become evident depends to some extent on where the distribution is centered. For example, for distributions centered at $\alpha = 50$, the agreement begins to fail beyond $\theta = 4°$; for distributions centered at $\alpha = 30$, the discrepancy occurs beyond $\theta = 5°$. This behavior can be explained by considering that the Fraunhofer approximation anticipates an inverse functional dependence between particle size and scattering angle. Furthermore the angular region in which both formalisms give identical results is that governed by the paraxial approximation $\sin\theta \approx \theta$, implicit in the characteristic Airy pattern.

The similarity between intensity patterns produced by the three distributions defined within a similar region of particle size eliminates any hypothesis that the critical region of validity of the Fraunhofer approximation is dependent on the type of distribution we use. This conclusion is further borne out by considering the same three distributions in regions beyond the critical size interval. For distributions defined within the interval $1 \leq \alpha \leq 60$, with modal peak in the interval $10 \leq \alpha \leq 30$, at least 68% (and occasionally up to 100%) of the particles that make up the distribution have a size parameter $\alpha \leq 45$. The result is different intensity patterns for each theory. If we shift the modal peak and the size interval for the distributions to greater sizes with respect to the critical interval, the intensity patterns coincide to within an angular interval $0° \leq \theta \leq 4°$, for distributions defined within the interval $30 \leq \alpha \leq 170$; whereas for distributions defined within the interval $50 \leq \alpha \leq 250$ the intensity patterns coincide for $0° \leq \theta \leq 2.5°$.

The previous discussion enables us to justify our selection of the interval $1 \leq \alpha \leq 100$, with corresponding modal values between $30 \leq \alpha \leq 50$ as being that which encompasses the limit of validity of the Fraunhofer approximation. In the following paragraphs we analyze the retrieved distributions obtained in this region.

In Figure 2 we compare the retrieved distributions obtained from the Fraunhofer approximation by us-

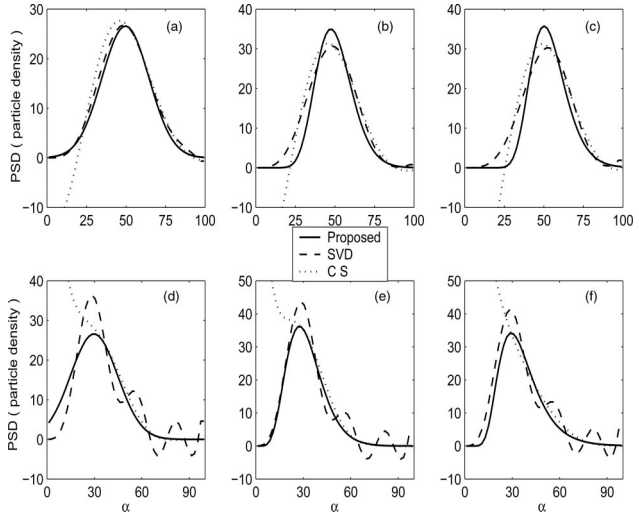

Fig. 2. Recovered distributions using the Fraunhofer approximation with the SVD and CS inversion methods. Graphs (a), (b), and (c) correspond to normal, gamma, and lognormal distributions, respectively, with modal peaks at $\alpha \sim 50$. Graphs (d), (e), and (f) as above, for $\alpha \sim 30$.

ing the CS and the SVD inversion methods. Figures 2(a) and 2(d) correspond to normal distributions, Figs. 2(b) and 2(e) are for gamma distributions, and Figs. 2(c) and 2(f) for lognormal distributions. Each pair of functions corresponds once again to the extremes of the critical size interval. We observe that for all distribution types SVD inversion generates superior results compared with CS.

It is well known that when working with the Fraunhofer approximation the retrieved distributions are strongly dependent on the angular composition of the scattered intensity, and to apply numerical techniques the sampling interval must be finite, $\theta_{min} \leq \theta \leq \theta_{max}$. Furthermore within this interval the aforementioned function must be discretized into a finite number of points. In the profiles discussed in this section, we use the same values of $\theta_{min} = 0.057°$, $\theta_{max} = 10°$, and $\Delta\theta = 0.057°$ throughout.

We find that the value of θ_{max} is critical for adequate retrieval of distributions using CS inversion. One must sample up to a value of θ_{max} that coincides with the angular region in which the intensity patterns produced by Mie and Fraunhofer formalisms begin to differ [see Figs. 1(b) and 1(d)]. If this is not the case then the retrieved function bears no resemblance whatsoever to that expected. Despite consideration of an adequate value for θ_{max}, in accordance with the paraxial condition that gives rise to the Fraunhofer approximation, we observe that the retrieved function continues to present considerable noise in the region corresponding to small particle size, for each of the three distribution types. This noise may be attributed to an incompatibility between the intervals of Eqs. (7) and (8) as mentioned previously. For this reason, we reject the employment of the retrieval method using the CS inversion in our subsequent analysis of the critical interval of validity of the Fraunhofer approximation, making a final comment that this inversion method is suitable in the region of large particle sizes.

A retrieval using the SVD method also depends on the correct selection of θ_{max}, although in this case the dependence is not so clearly evident. If the recuperation is carried out considering the totality of singular values, we obtain a result similar to that obtained when CS inversion is employed with an inadequate value of θ_{max}. The retrieved functions improve dramatically, however, when we begin to eliminate (replace with zeros) the smallest singular values in the linear system of equations. We may interpret this as a diminishment in θ_{max} and a simultaneous improvement in the conditioning of the matrix to be inverted, since if for the same distribution we calculate the intensity by using an adequate value of θ_{max}, then the number of singular values that must be eliminated is less than in the previous case, and the condition number of the matrix is reduced. The same behavior of improvement in the matrix conditioning is observed when the sampling ratio $\Delta\theta$ diminishes; however, an analysis of this effect is not intended to form part of this paper.

Although no formula exists for determining the number of singular values that must be removed, the retrieved functions obtained by varying this parameter to obtain the optimum results show that the SVD method is adequate for our present analysis. For the three types of distribution, with modal peaks in the region $\alpha = 50$, acceptable results are obtained by using SVD [see Figs. 2(a)–2(c)]. Meanwhile distributions with modal peaks in the region $\alpha = 30$ exhibit noise [see Figs. 2(d)–2(f)], which is manifested as oscillations superimposed upon the proposed distribution. This behavior is attributable in large part to the inadequacy of the Fraunhofer approximation in the inversion process for the given size interval and, to a lesser extent, to the asymmetry of the proposed distributions.

Since the behavior is similar for each type of distribution, both in the intensity patterns and in the inversions, we continue our analysis in this section only with normal distributions. At the same time we further limit the interval of modal size in the distributions so as to obtain an indicative limiting value for the Fraunhofer approximation. We consider a series of six normal distributions centered at $\alpha = 48, 47, 46, 44, 43, 42$, since by observation we note that in this region of mean size parameter, the Fraunhofer approximation loses its validity. Each distribution has the same sampling as before (see the caption of Table 1), and the SVD inversion method is employed throughout. The retrieval of this series of distributions using SVD is shown in Fig. 3.

As an indicator of error between the proposed and the retrieved distributions, we take the standard deviation

$$s = \frac{1}{N_s}\sqrt{\sum_{i=1}^{N_s}\frac{(f_i - x_i)^2}{f_i^2}}, \tag{16}$$

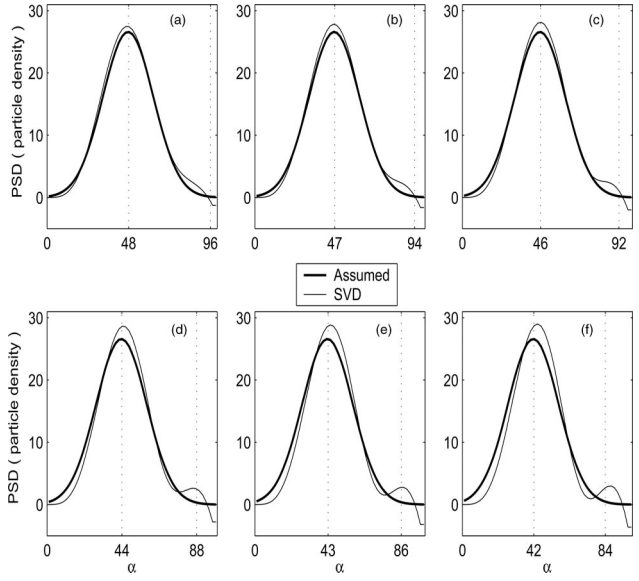

Fig. 3. Normal distributions recovered using the Fraunhofer approximation with the SVD inversion method in the critical size interval.

where f_i and x_i, are the i values of the proposed and the retrieved distributions, respectively, and N_s is the number of points calculated. The error values are 0.86, 0.92, 1.06, 1.59, 1.94, and 2.32 for Figs. 3(a)–3(f), respectively.

These results allow us to confirm that for the Fraunhofer approximation a critical interval exists for the modal peak of distributions centered between size parameter $42 \leq \alpha \leq 48$. We can consider the distribution centered at $\alpha = 46$ [Fig. 3(c)], as best representing the threshold value of validity for the Fraunhofer approximation, applied to recuperate smooth distributions of types such as normal, gamma, and lognormal. We can conclude that, for monomodal distributions with modal size parameters greater than the threshold value ($\alpha = 46$) with errors less than unity and employment of the SVD inversion method, it is clearly convenient to use the Fraunhofer approximation. Conversely, for monomodal distributions with modal size parameters below this threshold value, we propose the use of Mie theory.

5. Mie Theory: Comparison between Singular Value Decomposition and Phillips–Twomey

For distribution retrieval using Mie theory, we use both the SVD and PT inversion methods, with the three distribution pairs considered at the extremes of the Fraunhofer interval of validity as defined in the previous section. The plots are shown in Fig. 4, with associated errors in Table 2. Retrieval using SVD is clearly inferior, exhibiting incorrectly centered modal peaks and excessive noise, while the PT method shows evident superiority. For the latter we used a regularization parameter $\gamma = 10^{-18}$, selected in agreement with Eq. (15). In Section 6 we discuss the importance of this parameter to obtain optimal results.

Table 2. Error in the Retrieval of Fig. 4 using PT and SVD Methods with Mie Theory

Figure	Distribution	Modal Peak	Error PT	Error SVD
4(a)	Normal	50	1.54	2.0
4(b)	Gamma	~50	1.42	4.72
4(c)	Lognormal	~50	1.21	4.75
4(d)	Normal	30	1.17	9.25
4(e)	Gamma	~30	4.08	10.05
4(f)	Lognormal	~30	4.37	8.57

The poor performance of SVD with Mie theory may be largely attributed to the instability of the scattering matrix as reflected by a large condition number, which can be used as a measure of the degree of ill-posedness in the inverse problem. The matrices generated in the numerical calculations of Fig. 4 produce a condition number of 1.56×10^{21}, which when combined with the asymmetry of the proposed distributions makes second-order normalization a necessity, as in the case of the PT method. In other words, first-order normalization methods such as SVD[12] cease to be adequate in highly unstable inversion problems. For example, in the distributions of Section 4 (Fig. 3), where the scattering matrices were constructed using the Fraunhofer approximation, the SVD method was successful, since here the condition number was 2 orders of magnitude lower (5.85×10^{19}).

The second reason for the poor performance of the SVD method with Mie theory is the asymmetric shape of the proposed distributions. For example, despite using the same condition number throughout, the symmetric distribution of Fig. 4(a) produces better results than the asymmetric distribution of Fig. 4(f).

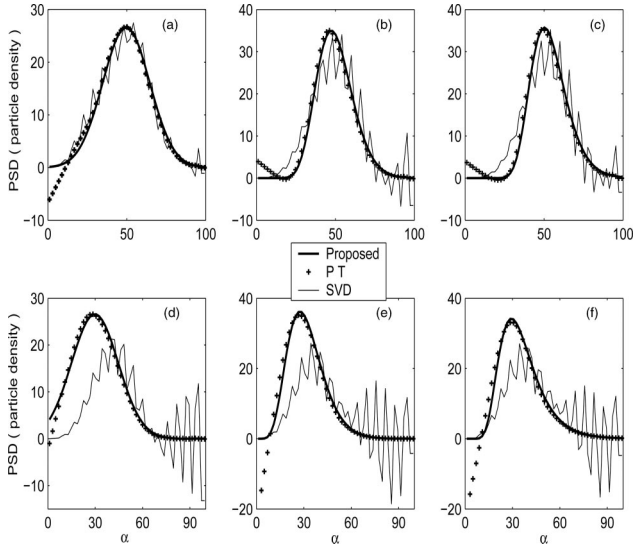

Fig. 4. Distributions recovered using Mie theory with the PT and SVD inversion methods. The regularization parameter $\gamma = 10^{-18}$ is used throughout. Graphs (a), (d), (b), (e), and (c), (f) correspond to the normal, gamma and lognormal distributions, respectively.

With regard to the use of the PT method with Mie theory, the asymmetry in the distributions has little effect on the ability of this method to recover the proposed distributions. Although the error for PT is almost tripled for the distributions with the highest asymmetry [gamma and lognormal with modal peak $\alpha \sim 30$; see Figs. 4(e) and 4(f), respectively], the removal of the negative (nonphysical) values from the analysis reduces the error to unity or less.

From the results presented in this section, we may thus conclude that the SVD inversion method is less than adequate when used with Mie theory, while the PT method, for the three kinds of asymmetrical distributions considered here, gives acceptable results, especially if we discard nonphysical (negative) values in the retrieved profile. Based on these observations, we expand our analysis in the following sections to regions of large and small particle size, exclusively for one kind of distribution.

6. Phillips–Twomey Method and the Optimal Regularization Parameter

When we use Mie theory with the PT method, an important aspect to be taken into account for solving the inverse problem is the proper choice of the regularization parameter to obtain optimal results in the retrieved distribution. Two different approaches commonly exist for making this selection. The first is based on an iterative process and can be applied in any situation since no estimation of noise level in the input data is needed. This iterative procedure is robust and gives good estimations of the sought distribution. In the second approach more information is needed and no iteration is required. However, it is necessary to assume some restrictions on both the expected solution and the noise of the measurements since they affect the quality of the solution. Thus the application of this last approach may be more difficult.

As already mentioned in Section 3, we use the iterative procedure for the selection of the regularization parameter. Taking γ_0 given by Eq. (15) as an initial value guarantees that we are on the path toward a practical solution. The selection of this initial value accelerates the convergence of the iterative process and reduces the number of steps to reach an optimal value γ_{opt}. We propose that γ_{opt} is reached when the error between the recovered and the proposed distribution is a minimum.

Figure 5 shows the evolution of parameter γ for two gamma distributions of several particle sizes. We show two different distributions to illustrate the challenges involved in the procedure for proper selection of γ_{opt}. The first is representative of distributions in the region of large particles where the Fraunhofer approximation can be applied. The second is for the regime of small particle sizes where Mie Theory is adequate. We have explored the solutions obtained for different values of γ but report here only the distributions that correspond to the initial and optimal values of the regularization parameters.

For the larger particles [Fig. 5(a)], the regularization parameter has an initial value given by $\gamma_0 = 5.9938 \times 10^{-11}$, represented by the symbol $\varnothing$ in Fig. 5(b). This gives a retrieved distribution with an error of 1.6057, appearing in Fig. 5(a) as a dashed curve. After several steps an optimal value $\gamma_{opt} = 5.9938 \times 10^{-15}$ is obtained as indicated by the symbol $\oplus$ in Fig. 5(b). This gives a retrieved distribution with an error of 0.2797, corresponding to the thin solid curve in Fig. 5(a). However, this last plot is not well distinguished since it coincides with the proposed distribution.

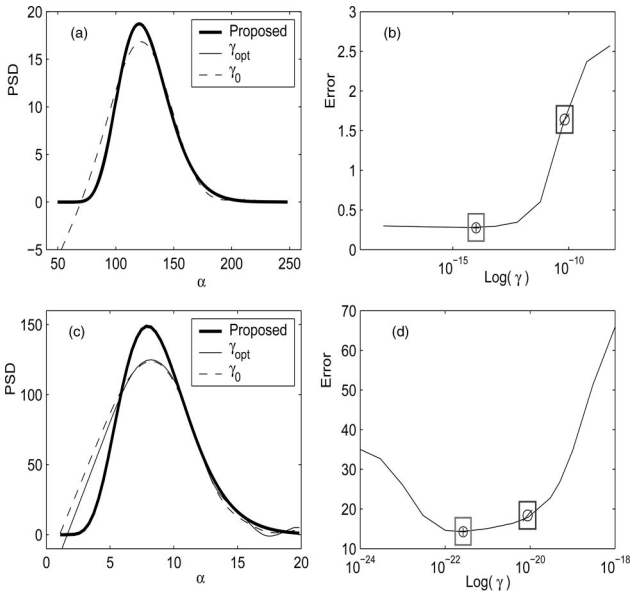

Fig. 5. Evolution of the regularization parameter. Plots (a) and (c) are the distributions retrieved with values of γ_0 and γ_{opt}, respectively. In (b) the values of $\gamma_0 = 5.9938 \times 10^{-11}$ ($\varnothing$) and $\gamma_{opt} = 5.9938 \times 10^{-15}$ ($\oplus$) generate the distributions of the large particles shown in (a). Similarly in (d), the values $\gamma_0 = 9.0564 \times 10^{-21}$ ($\varnothing$) and $\gamma_{opt} = 2.0 \times 10^{-22}$ ($\oplus$) generate the distributions for the small particles shown in (c).

For the small particles [Fig. 5(c)], the initial value is $\gamma_0 = 9.0564 \times 10^{-21}$, also represented by $\varnothing$ in Fig. 5(d), and the corresponding retrieved distribution has an error of 17.9142. The optimal value of the regularization parameter is $\gamma_{opt} = 2.0 \times 10^{-22}$ represented by the symbol $\oplus$ in Fig. 5(d), with an error between the proposed and the retrieved distribution given by 14.3582. In this case also the retrieved distributions [Fig. 5(c)] are represented by a dashed curve for the initial value of γ, and a thin curve for the optimal value of γ.

We can see that γ_{opt} provides adequate results for large particles with good agreement between the proposed and the recovered distributions, since the error is less than unity. However, for the region of small particle size, the reconstructed distribution is degraded in spite of selecting the optimal value of γ. This is typical in a very narrow distribution, where, as the distribution gets wider, the recovery improves. Similar results are obtained with narrow normal and lognormal distributions.

Since the scattering matrix condition number used in the SVD method can be used as a measure of the degree of ill-posedness, we have tried to find a rela-

tionship between this condition number and the optimal regularization parameter but without success.

In summary, we show that the application of this iterative procedure to select the regularization parameter gives optimal values. In general, good estimations of the retrieved distributions are obtained by using the PT method. The process works well for broad distributions with large particles, but fails somewhat for narrow distributions skewed toward small particle sizes. The performance of this method demands a considerable amount of computing time.

7. Comparison of Mie Theory and the Fraunhofer Approximation

We now consider the comparison of the reconstruction of a normal distribution of large particles using Mie theory with the PT method and that reconstructed with the Fraunhofer approximation using both SVD and CS methods. The proposed distribution is defined in the interval $50 \leq \alpha \leq 250$, centered at $\alpha = 150$ and deviation $\sigma = 30$. The intensity pattern is calculated according to Mie theory, with $m = 1.5$ and $\lambda = 0.6328$ μm, for the angular resolution ($\Delta\theta$) shown in Table 1. This kind of distribution is intentionally chosen with the object of highlighting the unnecessary applicability of the Mie theory for very large spherical particles.

Figure 6 shows the performance of the three methods. The proposed distribution is represented by the continuous thick curve. The reconstructed size distribution with cross marks corresponds to Mie theory with the PT method, using the optimum value of regularization parameter, $\gamma = 1.0 \times 10^{-12}$. Obviously, with a very small value of error equal to 0.1598 and practically identical to the proposed distribution, this reconstruction can be considered acceptable.

The plots shown by the dashed curve and the dotted curve correspond to the Fraunhofer approximation with the SVD and the CS methods, respectively. Qualitatively speaking, the plot for SVD fits better to the proposed distribution, with an error of 0.9759, compared with an error of 2.5809 for CS. The peak of the plot for CS is better aligned to that of the proposed distribution, while the SVD peak is lightly shifted toward smaller α's . Additionally, the plot for CS is very noisy in the small size region, and this may be associated with the truncation of the numeric integral at some cutoff angle θ_{max}, while the negative number density is due to the missing data at small angles of the scattering pattern. Meanwhile the plot for SVD shows a slight disagreement with the proposed distribution at extremes of small and large particle sizes. This is possibly due to the discretization of the data in the scattering matrix and may also be due to a bad selection of the angular sampling interval. These incompatible conditions for the Fraunhofer approximation with both methods result in a poor inversion performance compared with the Mie theory using the PT method. Nevertheless, we maintain that the Fraunhofer approximation has a practical use for some applications, i.e., when the problem involves particles with unknown refractive indices and has practical measurement limitations, or simply when the main objective is to reduce computing time.

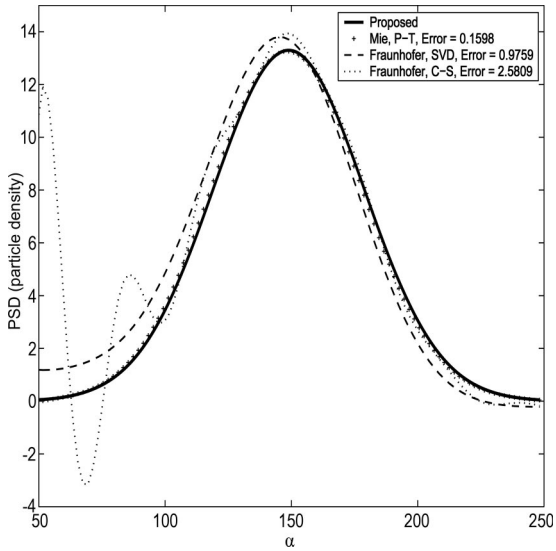

Fig. 6. Comparison between Mie theory and the Fraunhofer approximation in the region of large particle sizes.

Finally, we state that Mie theory with PT inversion provides superior results when compared with the Fraunhofer approximation using either CS or SVD algorithms, the first combination of methods exhibiting the lowest error. However, it must also be noted that retrieval using Mie theory requires a factor of 4500 more CPU time than the method using the Fraunhofer approximation. For this reason, we suggest using Mie theory with the PT method only for distributions under the threshold value for the validity of the Fraunhofer approximation.

8. Conclusions

For smooth, normal, gamma, and lognormal, monomodal particle-size distributions composed of spherical particles, with real relative refractive indices given by $m = 1.5$, it is appropriate to use the Fraunhofer approximation beyond a certain critical size interval. This interval corresponds to the modal peak of the distribution centered between $42 \leq \alpha \leq 48$. We consider the distribution centered at $\alpha = 46$ as best representing the threshold value for the validity of the Fraunhofer approximation. Additionally, the method of singular value decomposition generates better results than the Chin–Shifrin method when solving the inverse problem with the Fraunhofer approximation. In this part of the work all the distributions were considered in the size dominium between $1 \leq \alpha \leq 100$.

The singular value decomposition inversion method produces unacceptable results when used with Mie theory, while the Phillips–Twomey method gives the best results for all three kinds of distribution considered here. The asymmetric shape of the distribution does not affect the efficiency of the Phillips–Twomey method. We also note that a larger sampling interval has no effect on the performance of this method.

The principal factor that affects the success of the Phillips–Twomey method is the regularization parameter. The application of an iterative procedure to select this parameter gives an optimal value that produces a good estimation of the retrieved distribution. This optimal value produces an error of less than 1 for broad distributions with large particles, but the retrieved distribution is not so accurate for narrow particle distributions skewed toward small sizes. The performance of this method demands a considerable amount of computing time.

With regard to comparison of the Mie and Fraunhofer formalisms within the region of large particle sizes where the use of the Fraunhofer approximation is perfectly valid, we can conclude that the combination of Mie theory with the Phillips–Twomey method results in a better approach compared with singular value decomposition and the Chin–Shifrin method using the Fraunhofer approximation. The only disadvantage of Mie theory in this case is an increase in CPU time by 4 orders of magnitude. Hence we recommend using the Fraunhofer approximation with the singular value decomposition inversion method.

This study was conducted while J. Vargas-Ubera was at the Benemérita Universidad Autónoma de Puebla, Facultad de Ciencias Físico-Matemáticas. The permission to undertake doctoral studies is gratefully acknowledged. The authors thank the Mexican National Council for Science and Technology (Conacyt) for a doctoral fellowship and acknowledge the partial support received from INAOE and the Mexican Institute of Petroleum (IMP).

References

1. H. C. van de Hulst, *Light Scattering by Small Particles,* 2nd ed. (Dover 1981).
2. J. R. Hodkinson, "Particle sizing by means of the forward scattering lobe," Appl. Opt. **5,** 839–844 (1966).
3. A. R. Jones, "Error contour charts relevant to particle sizing by forward-scattered lobe methods," J. Phys. D **10,** L163–L165 (1977).
4. A. L. Fymat, "Analytical inversions in remote sensing of particle size distributions. 2: Angular and spectral scattering in diffraction approximations," Appl. Opt. **17,** 1677–1678 (1978).
5. J. Liu, "Essential parameters in particle sizing by integral transform inversions," Appl. Opt. **36,** 5535–5545 (1997).
6. J. H. Koo and E. D. Hirleman, "Synthesis of integral transform solutions for the reconstruction of particle-size distributions from forward-scattered light," Appl. Opt. **31,** 2130–2140 (1992).
7. S. D. Coston and N. George, "Particle sizing by inversion of the optical transform pattern," Appl. Opt. **30,** 4785–4794 (1991).
8. J. C. Knight, D. Ball, and G. N. Robertson, "Analytical inversion for laser diffraction spectrometry giving improved resolution and accuracy in size distribution," Appl. Opt. **30,** 4795–4799 (1991).
9. J. B. Riley and Y. C. Agrawal, "Sampling and inversion of data in diffraction particle sizing," Appl. Opt. **30,** 4800–4817 (1991).
10. L. C. Chow and C. L. Tien, "Inversion techniques for determining the droplet size distribution in clouds: numerical examination," Appl. Opt. **15,** 378–383 (1976).
11. E. D. Hirleman, "Optimal scaling of the inverse Fraunhofer diffraction particle sizing problem: the linear system produced by quadrature," Part. Part. Syst. Charact. **4,** 128–133 (1987).
12. W. H. Press, S. A. Teukolsky, W. T. Vetterling, and B. P. Flannery, *Numerical Recipes in Fortran: the Art of Scientific Computing,* 2nd ed. (Cambridge U. Press, 1992).
13. S. Twomey, "On the numerical solution of Fredholm integral equations of the first kind by inversion of the linear system produced by quadrature," J. Assoc. Comput. Mach. **10,** 97–101 (1963).
14. D. A. Ligon, T. W. Chen, and J. B. Gillespie, "Determination of aerosol parameters from light-scattering data using an inverse Monte Carlo technique," Appl. Opt. **35,** 4297–4303 (1996).
15. N. S. Mera, L. Elliott, and D. B. Ingham, "On the use of genetic algorithms for solving ill-posed problems," Inverse Probl. Eng. **11,** 105–121 (2003).
16. M. Ye, S. Wang, Y. Lu, T. Hu, Z. Zhu, and Y. Xu, "Inversion of particle-size distribution from angular light-scattering data with genetic algorithms," Appl. Opt. **38,** 2677–2685 (1999).
17. S. D. Coston and N. George, "Recovery of particle-size distributions by inversion of the optical transform intensity," Opt. Lett. **16,** 1918–1920 (1991).